

FZK-176-1

GD

NUCLEAR AEROSPACE RESEARCH FACILITY

21 DECEMBER 1963

**MONTE CARLO CALCULATIONS
OF ENERGY DEPOSITIONS
AND RADIATION TRANSPORT**

Volume 1: Validation of COHORT Codes

D. G. Collins
T. W. DeVries

Contract No. NAS8-5182

Work performed for
National Aeronautic and Space Administration
under the technical direction of
George C. Marshall Space Flight Center
Huntsville, Alabama

GENERAL DYNAMICS | FORT WORTH

FOREWORD

This is the first of a two-volume report on the COHORT (Calculation of Heating or Radiation Transport) codes. The work was performed at the General Dynamics/Fort Worth Nuclear Aerospace Research Facility (NARF), under Contract NAS8-5182 with the National Aeronautics and Space Administration, George C. Marshall Space Flight Center, Huntsville, Alabama. The work consisted of the checkout of seven Monte Carlo codes developed under a previous contract (NAS8-1573).

This volume of the report contains comparisons of the COHORT data with other calculational and experimental data. The second volume gives listings of the FORTRAN statements for the seven codes, the input-data formats, and instructions for utilizing the codes.

ABSTRACT

27941

A Monte Carlo procedure for the IBM-7090 digital computer has been developed to perform calculations of the radiation heating in propellant tanks and the radiation environment about a nuclear rocket stage. The procedure is made up of seven codes. These codes generate primary-source-particle parameters, neutron and gamma-ray histories, and secondary-gamma-ray source parameters. The codes will also analyze the history data so that the particular quantities desired as answers to a given problem may be determined.

The results from the Monte Carlo codes are compared with other calculations of the heat deposition in liquid hydrogen and with calculations and measurements of the angular distribution of a fast-neutron dose rate transmitted through a 9-inch polyethylene slab. Information reported includes sources of the cross-section data gathered in preparation for a flux leakage calculation from a NERVA-type engine.

CONTENTS

	Page
FOREWORD	ii
ABSTRACT	iii
LIST OF FIGURES	v
I. INTRODUCTION	1
II. COMPARISON OF RESULTS WITH OTHER DATA	4
2.1 Energy Deposition in Liquid Hydrogen	4
2.2 Comparison of Angular Distribution of Dose Rates Leaking Through a Nine-Inch Polyethylene Slab	16
III. CALCULATIONS FOR NERVA-TYPE GEOMETRY	18
IV. RECOMMENDATIONS	21
REFERENCES	23
DISTRIBUTION	24

LIST OF FIGURES

Figure		Page
1	Neutron Heat Deposition versus Depth in Liquid-Hydrogen Slab from a 7-Mev Plane Source - Neutrons Incident Normal to Slab Surface	5
2	Gamma Heat Deposition versus Depth in Liquid-Hydrogen Slab from an 8-Mev Plane Source - Gamma Rays Incident Normal to Slab Surface	7
3	Neutron Heat Deposition in a Liquid-Hydrogen Cylinder from a 3-Mev Point Isotropic Source	9
4	Experimental Geometry - Plan View	11
5	Comparison of Calculated and Measured Fast-Neutron Flux Distribution Through a Nine-Inch-Thick Polyethylene Slab	13
6	Source-Term Spectrum	14
7	Comparison of Angular Distributions of Scattered-Neutron Dose Rates Through a Nine-Inch-Thick Polyethylene Slab	16

I. INTRODUCTION

The proposed use of a cryogenic liquid as a propulsion agent for a nuclear rocket system has emphasized the need for more refined methods of calculating radiation transport and nuclear energy depositions. Nuclear heating in cryogenic fuel may pose a serious problem because of the increase in vapor pressure associated with the rise in temperature effected by the deposited energy. Shielding of the propellant tanks, of course, could lessen the amount of energy deposited in the fuel through a reduction in the intensity of radiation incident upon the tank. However, the addition of shielding materials to a rocket system is undesirable because of the weight added to the system. The addition of shielding materials to reduce the neutron flux incident upon the propellant tank may also result in an increase in the gamma-ray flux due to capture and inelastic gamma rays produced in the shield. It has become important, therefore, that rigorous methods of analyzing all phases of radiation transport and energy deposition for complex rocket geometries be developed.

A set of seven IBM-7090 machine codes has been developed for the analysis of radiation transport within complex geometries, such as those that may be encountered in a study of nuclear rocketry, and for the calculation of nuclear energy depositions in fuel and in structural and shield materials.

These codes, developed at General Dynamics/Fort Worth, are referred to collectively as the COHORT (Calculation Of Heating Or Radiation Transport) procedure. They are applicable to more than just nuclear rocket calculations and may prove to be of value in many other areas of radiation transport studies.

The COHORT procedure consists of seven codes: (1) the Primary-Source Generation Code, (2) the History-Generator Code, (3) the Tape-Sort Code, (4) the Analysis Code "A01," (5) the Analysis Code "A02," (6) the Secondary-Source-Generation Code, and (7) the Tape-Read Code. Instructions for using each of these codes are given in Volume II of this report.

The development of the COHORT codes began under a previous contract and a report (Ref. 1) written at the completion of that contract describes in detail much of the mechanics of the various calculations performed by the codes. Volume II of this report is essentially an updating and reorganization of information contained in Reference 1. Several changes were made in the codes during the checkout phase, some of which effect a change in the formulae and wording of Reference 1. Most of the changes made were simply correction of errors found in the FORTRAN statements, but in a few instances changes were made in the original concepts. These changes were made either to simplify the mechanics of the codes, to substitute what was felt to be a more desirable approach, or to make the codes compatible with one another. Volume II, then, should be considered a replacement for the former report (Ref. 1), since

any changes made in the codes that affect the formulae or wording in Reference 1 are corrected in Volume II.

The first volume of this report pertains to calculations performed using the COHORT codes. These calculations were made, for the most part, to generate results to compare with those by other calculational models and thus to validate the COHORT codes. Three of the test problems involve energy deposition in liquid hydrogen, since this is the cryogenic liquid currently advanced as the propulsion agent for nuclear-powered rockets. Other test problems involved a calculation of the flux distribution within a 9-inch polyethylene slab and of the angular distribution of the dose rates leaking from the slab. These problems were run because of the good experimental and analytical data available for comparison. Because the codes treat scattering with hydrogen in a special manner, it was also desirable to have comparisons of calculations involving materials other than hydrogen.

A planned analysis of radiation leakages from a complex geometry describing a nuclear rocket engine was not possible, because of the delay encountered in checking out the COHORT codes. Cross sections and cumulative probability tables versus scattering angles were compiled for eight elements, and a geometry similar to the calculational model for the NERVA engine (Ref. 2) was described. An effort has been made to calculate the flux leakages from a NERVA-type engine. Although the results of this effort were not analyzed in time for inclusion in this report, work that has been completed is reported in Section III.

II. COMPARISONS OF RESULTS WITH OTHER DATA

2.1 Energy Deposition in Liquid Hydrogen

Calculations of the heating rates produced in liquid hydrogen by both neutron and gamma radiation were made in order to check the ability of the COHORT procedure to predict energy depositions. The heat deposition rates in liquid hydrogen calculated by Burrell (Ref. 3) were chosen for a standard of comparison. Burrell has calculated with a Monte Carlo model the heat deposition in liquid-hydrogen slabs and cylinders. For the slab geometries, plane, parallel-beam, monoenergetic neutron and gamma-ray sources incident at different angles to the slab face were considered. One of the quantities he calculated was the heat deposition as a function of depth into the liquid-hydrogen slab for each energy and each incident angle.

Figure 1 shows the comparison of the heat depositions shown in Reference 3 and those determined with the COHORT codes for a 7-Mev neutron source incident normal to a slab face. The agreement between the two sets of data is very good for all but the first few inches in the slab. This particular problem was run several times on the COHORT codes by varying the number of histories or the application of the exponential transformation on each run. The heat deposition in the first 5-10 inches of liquid hydrogen was consistently higher than that reported in Reference 3. Although the disagreement in the heat deposition for these first few inches of liquid hydrogen is not sufficient in magnitude to indicate any errors in the COHORT calculations, there

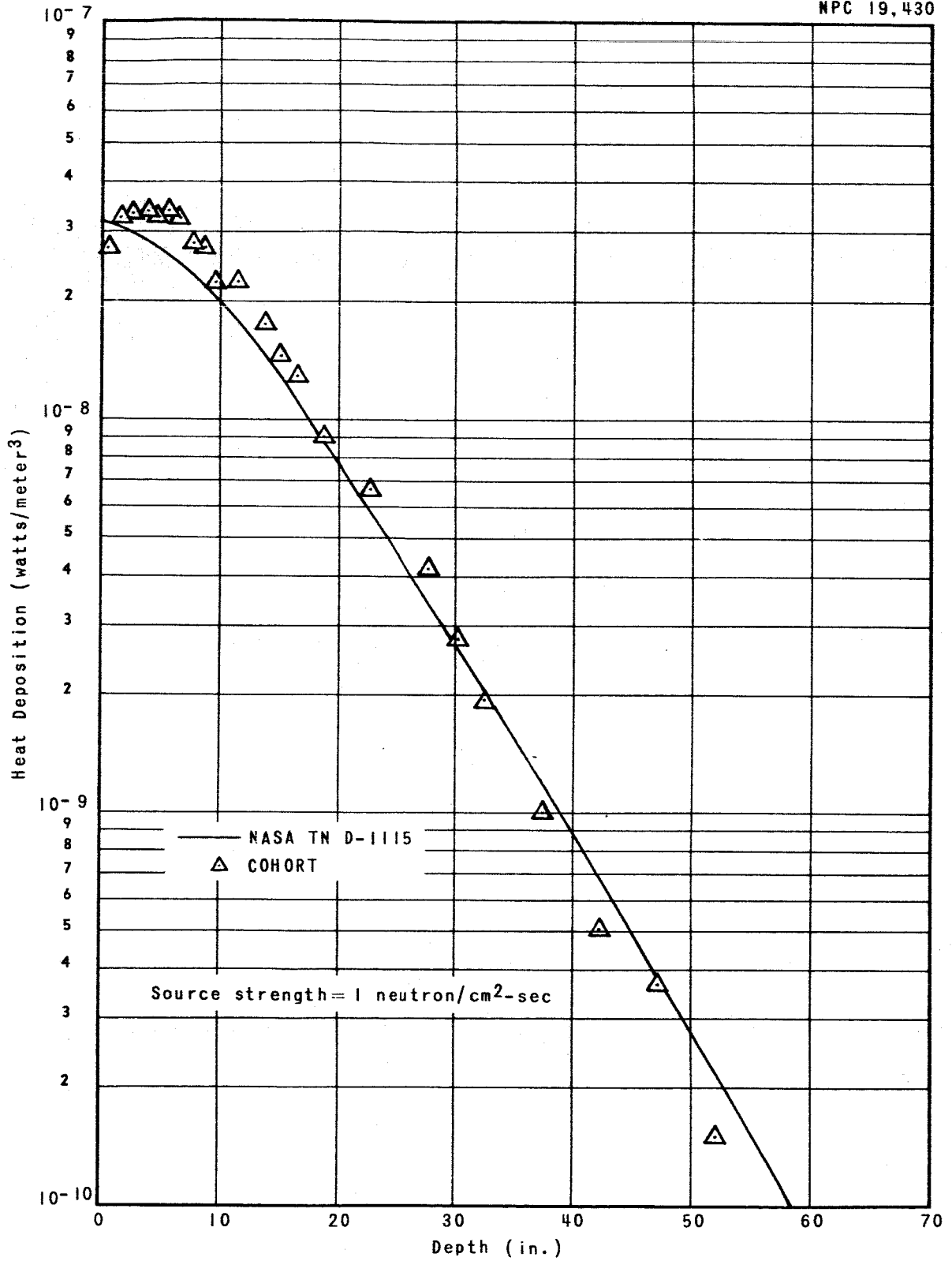


Figure 1. Neutron Heat Deposition versus Depth in Liquid-Hydrogen Slab from a 7-Mev Plane Source - Neutrons Incident Normal to Slab Surface

were some slight differences in the two calculations. As well as can be determined, the geometry and cross sections for the two calculations were the same; the COHORT results are based upon 4200 histories while the results of Reference 3 were based on 5000 or more histories. In the COHORT problem, histories were terminated when the energy dropped below 0.1 Mev; Reference 3 results were obtained for energies down to 1 ev. There was also a difference in the application of the exponential transformation. In Reference 3, the exponential transformation was applied only to the first path lengths; in addition, a biasing technique was applied to first path lengths to force a collision within the slab. The COHORT codes apply the same exponential transformation to all path lengths and does not require that a first collision occur in the slab.

Figure 2 shows the comparison of the calculations of the heat deposited by 8-Mev gamma rays incident normal to a liquid-hydrogen slab. Again, the comparison is with data calculated by Burrell. However, since the COHORT results are based upon only 1400 histories, disagreement among the data is probably not as serious as Figure 2 would indicate. In fact, the data agree very well when the fact that the COHORT results are based upon only 1400 histories is considered. The slab thickness for the COHORT calculation was 76 feet, while that for the Reference 3 calculation was later determined to be at least 98 feet. This may explain in part the reason for the lower prediction by the COHORT codes at large depths into the slab. A portion of that flux leaking through the 76-foot slab should have been scattered

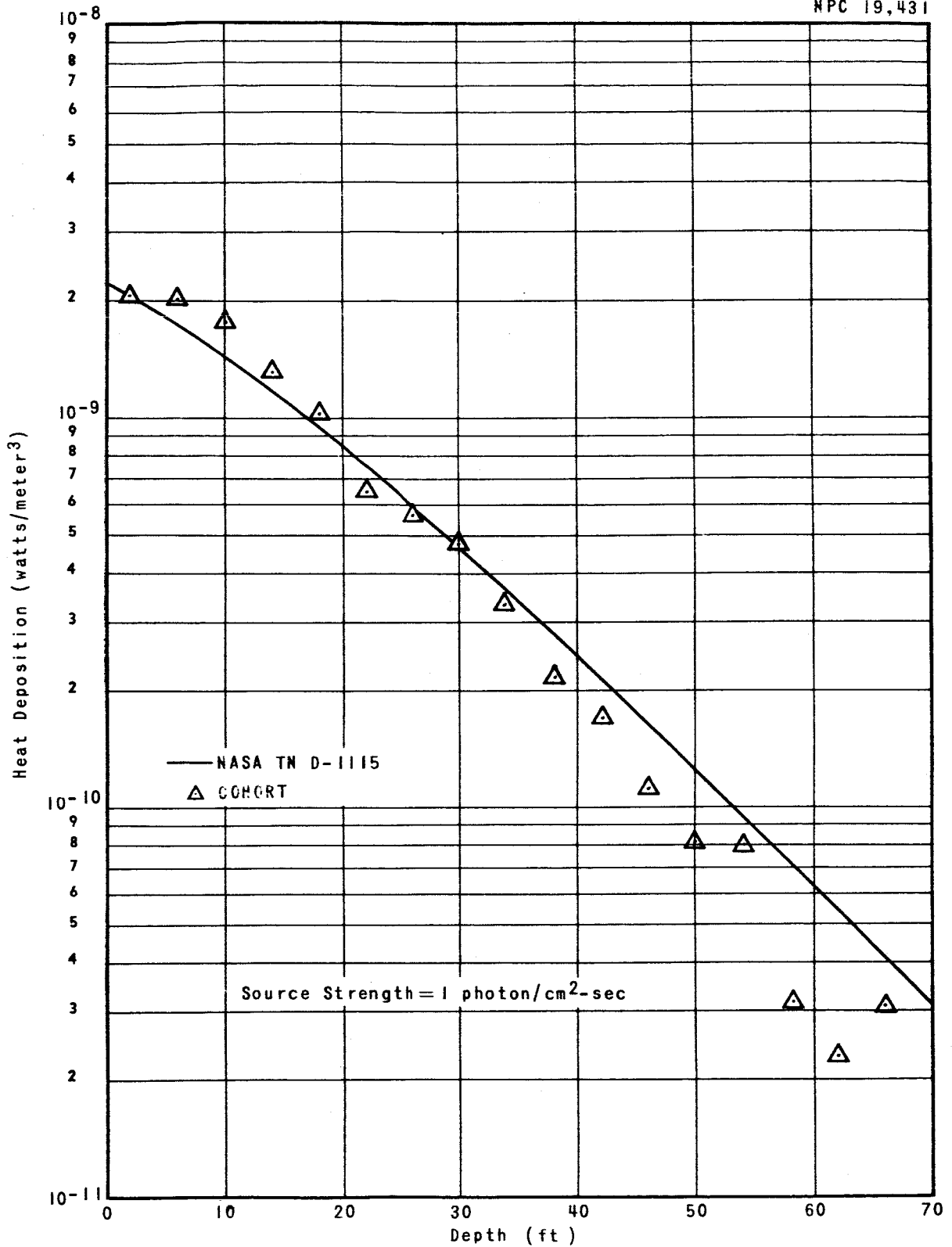


Figure 2. Gamma Heat Deposition versus Depth in Liquid-Hydrogen Slab from an 8-Mev Plane Source - Gamma Rays Incident Normal to Slab Surface

back and would have deposited more energy at the larger depths if the slab had been thicker. Gamma-ray cross sections were the same for both calculations. However, there was a slight difference in the application of the exponential transformation. In the COHORT calculation, path lengths were stretched to twice their normal lengths, and it is assumed that no biasing was used in the Reference 3 calculations.

The two calculations for the neutron and gamma-ray energy depositions should indicate the difference in the transport of neutrons and gamma rays through liquid hydrogen.

The third comparison made with data reported in Reference 3 was for heat deposition in a 30-foot-diameter liquid-hydrogen cylinder due to a 3-Mev point isotropic source located on the cylinder centerline 11.25 feet from the face of the cylinder (Fig. 3). The cylinder was divided into circular disks two inches thick and then each disk was divided into ten annular rings of equal volume. The heat deposited in the first 40 regions was calculated with the COHORT code and compared with the data in Reference 3. There were 2800 histories run with the COHORT code, and the result based upon that number of histories agree reasonably well with the data in Reference 3. The COHORT points appear to be slightly more erratic than those shown in the Figure 17 of Reference 3. This is probably due to the fewer number of histories run. It may be noted that the heat deposition was not calculated for as many volumes with the COHORT codes as it was in Reference 3. This was due to the limitation of the COHORT codes to 50 regions.

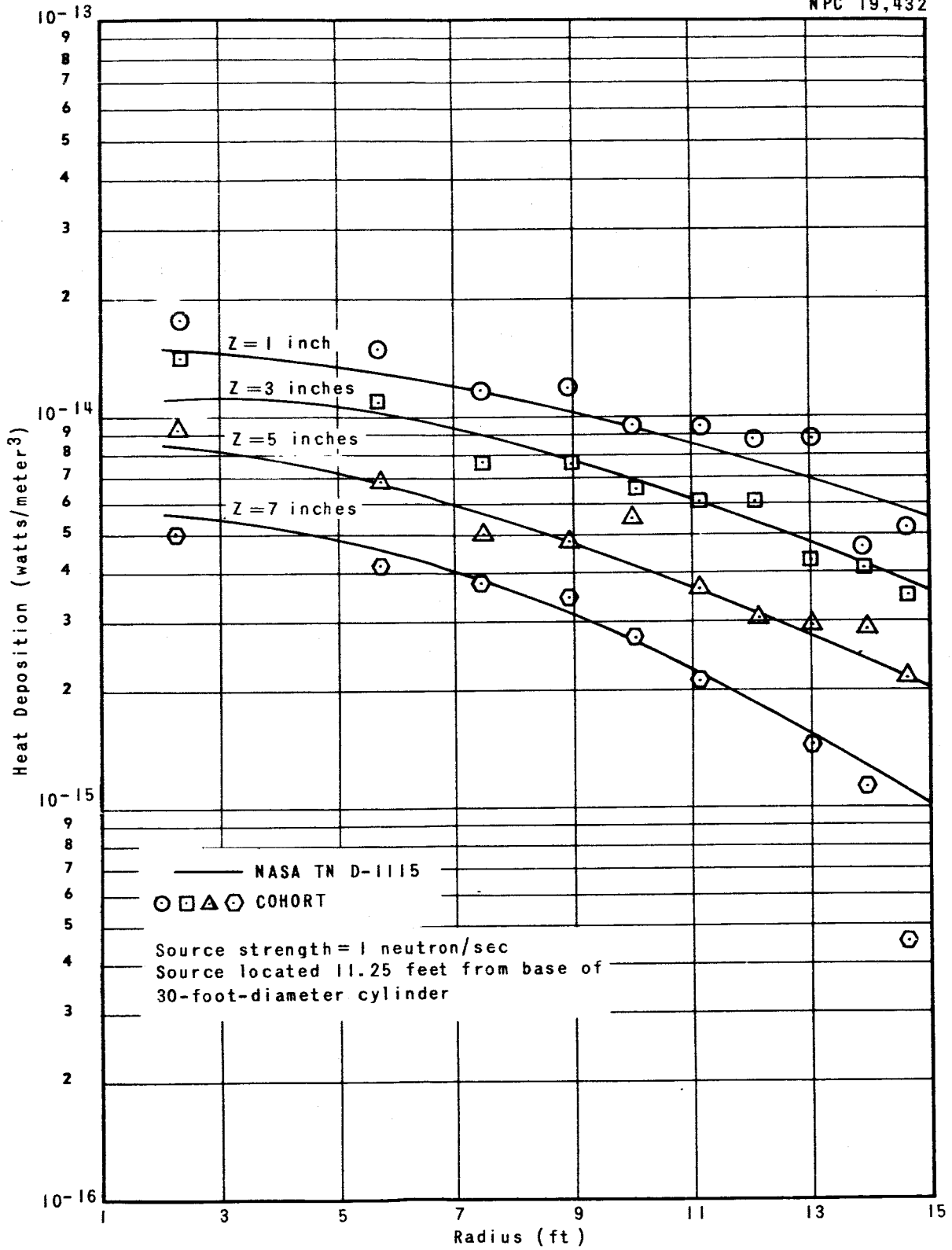


Figure 3. Neutron Heat Deposition in a Liquid-Hydrogen Cylinder from a 3-Mev Point Isotropic Source

The three comparisons of the heat depositions in liquid hydrogen were obtained without normalizing the COHORT results and do indicate that the code's ability to determine heat depositions is fairly reliable.

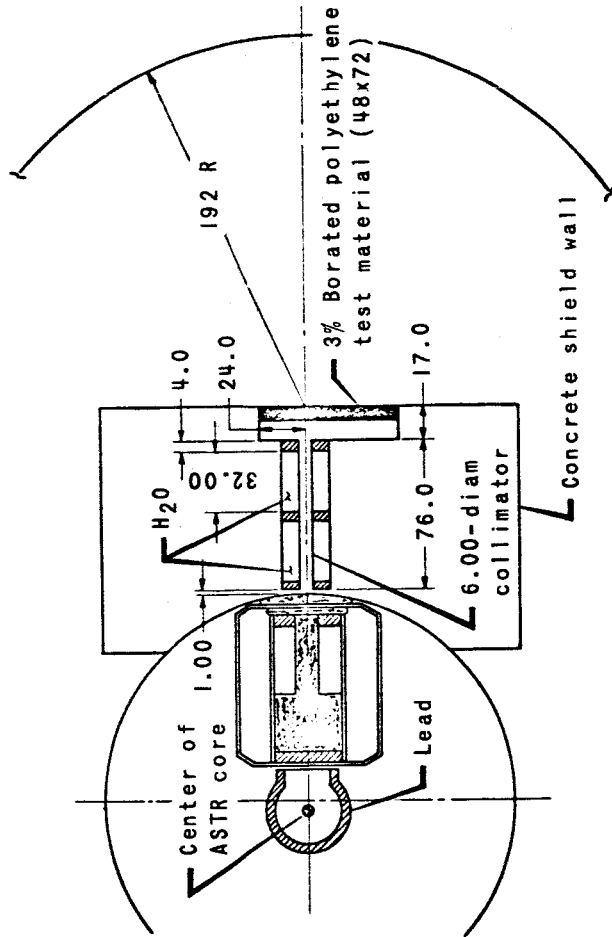
2.2 Comparison of Angular Distribution of Dose Rates Leaking Through a Nine-Inch Polyethylene Slab

Since the COHORT procedure treats scattering with hydrogen in special routines, comparisons with radiation transport calculations through a polyethylene slab were made to check out the other scattering routines. This particular geometry and material combination was chosen because of the availability of experimental and analytical data.

In the Angular and Energy Distribution Experiment recently conducted at the Nuclear Aerospace Research Facility (Ref. 4), measurements were taken of (1) the fast-neutron flux distribution in a 9-inch polyethylene slab, (2) the total fast-neutron leakage from the slab, and (3) the dose rate as a function of polar angle on an arc 192 inches from the slab center. Calculations to verify the experimental data were made with GD/FW's Monte Carlo slab penetration code C-18 (Ref. 5).

Preliminary requirements of the experimental geometry (Fig. 4) were that an infinite-slab condition be closely approximated and that radiation fluxes of sufficient intensity to obtain reliable data be available.

Following a series of preliminary investigations, it was determined that the experimental arrangement shown in Figure 4 would provide a satisfactory narrow-beam geometry in that an



All dimensions in inches

Figure 4. Experimental Geometry - Plan View

infinite-slab condition could be closely approximated. A map of the dose rates leaking through the slab showed the distribution to be highly peaked opposite the collimator and to be negligible at the outer extremities of the slab. Furthermore, the dimensions of the slab and the detector-slab separation distances were such that the detector "saw" that dose rate leaking from the slab as coming from one point.

Calculations were performed with the COHORT codes (1) to obtain the distribution of the flux above 2.9 Mev in the slab and (2) to predict the angular distribution of the dose rates emitted from the slab. Figure 5 shows the comparison of the COHORT calculation of the flux distribution with the experimental and C-18 calculation. Only 1400 histories were run for the COHORT problem, so that the results were not expected to agree any better than the agreement obtained.

There was some difficulty in obtaining the proper source term for the calculations, and the one now being used is not completely reliable. Reference 5 quotes a source term of 370 neutrons per second per watt incident upon the slab, but a comparison of the C-18 calculated data with experimental data shows that the flux above 2.9 Mev incident upon the slab was 370 neutrons/sec-watt. A quick check of the source spectrum (Fig. 6) will show that one third of the initial flux incident upon the slab is between 1.5 and 2.9 Mev. (The initial spectrum for the C-18 calculation ranged from 1.5 to 10 Mev.) The COHORT calculations in Figure 5 were multiplied by 555 neutrons/sec-watt, which was the calculated total source term, assuming that the source term for the initial flux above 2.9 Mev was 370 neutrons/sec-watt. The two calculations agree very well for about the first four

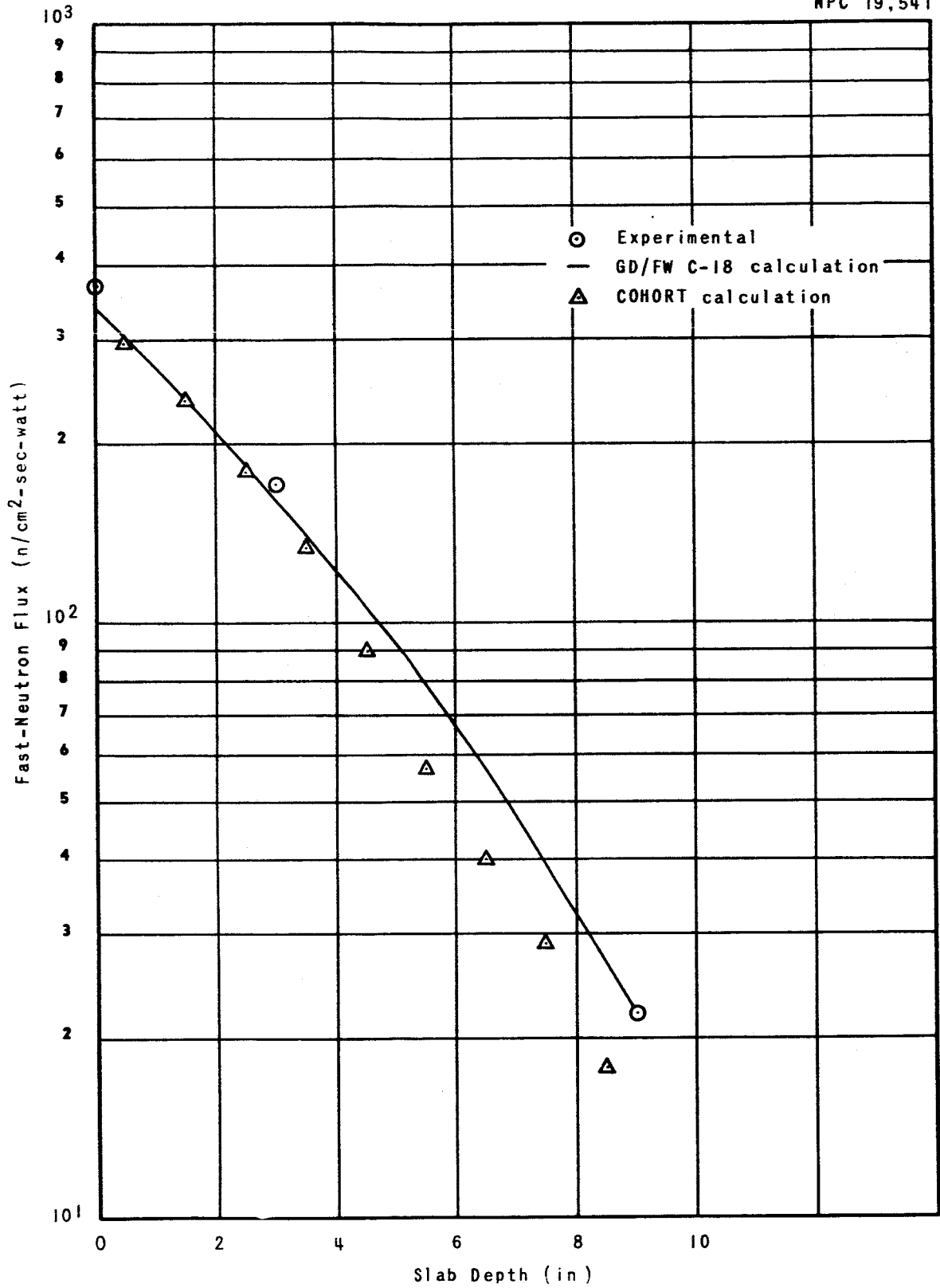


Figure 5. Comparison of Calculated and Measured Fast-Neutron Flux Distribution Through a Nine-Inch-Thick Polyethylene Slab

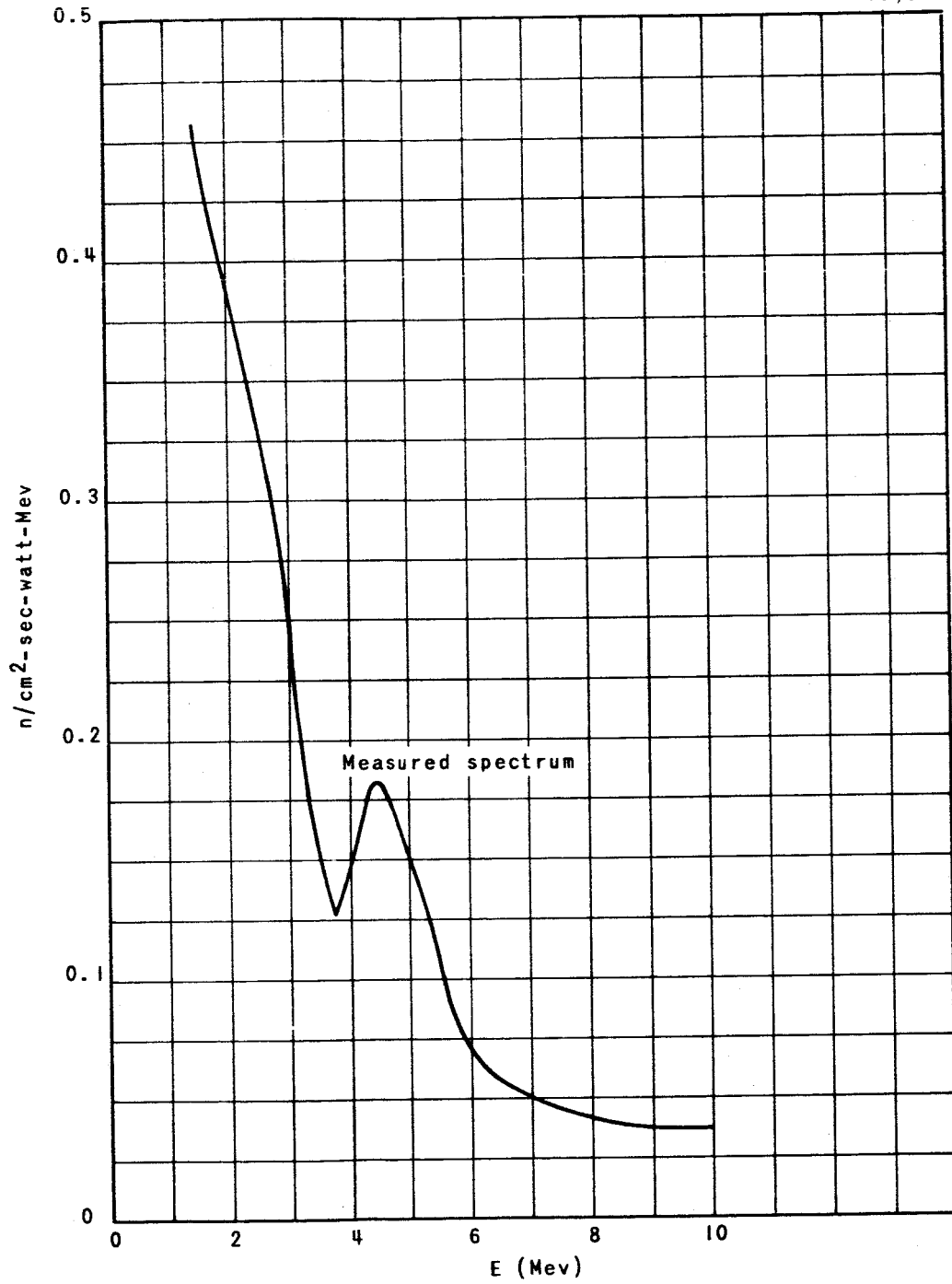


Figure 6. Source-Term Spectrum

inches into the slab, and then the COHORT results drop off more rapidly than the C-18 calculation. This may be due to the small number of histories run on the COHORT codes or possibly to the fact that no biasing was performed to improve the sampling in this portion of the slab. Both calculations under-predict the experimental points at the slab entrance, and this may be due to an improperly defined source term. It is to be noted that if the two calculations were normalized to the measured point at the zero thickness, the COHORT data would fit the experiment points about as well as the C-18 data.

In addition to a calculating of the flux distribution within the 9-inch polyethylene slab, the angular distribution of the dose rates leaking from the slab were also determined. The angular distribution of the dose rates were determined by measuring and calculating the dose rates at several points on a radius 192 inches from the center of the outer slab face. Figure 7 shows comparisons of the dose rates determined along the 192-inch radius for two COHORT calculations with a C-18 calculation that was reported to have accurately predicted the experimental data. (Ref. 5). The dashed curve and the histogram in Figure 7 are two different calculations made with the COHORT codes. The dashed curve was drawn through a set of five points, that represent the dose rates calculated at each of five detectors located on the 192-inch radius at angles of 0, 10, 25, 35, and 45 degrees. The histogram represents the dose rates obtained on the assumption that all the flux leaking through the slab appeared to be coming through at a single point. Thus, the dose rate for a detector of

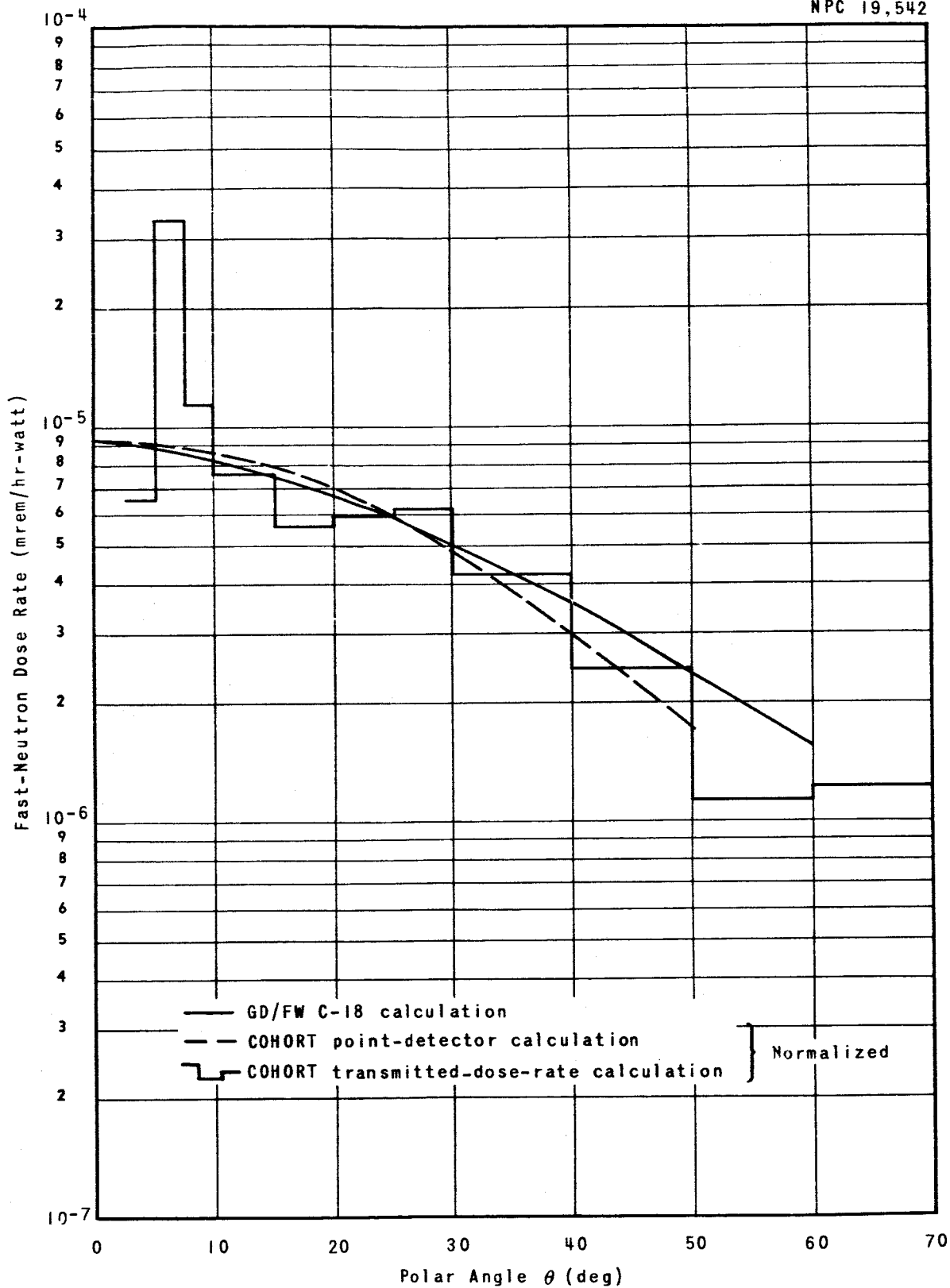


Figure 7. Comparison of Angular Distributions of Scattered-Neutron Dose Rates Through a Nine-Inch-Thick Polyethylene Slab

unit area located 192 inches away was obtained by multiplying the dose rate per steradian leaking through the slab by the solid angle subtended by the detector. The dose rates calculated with the C-18 code were obtained in like manner, since the C-18 code also gives the flux or number current at the outer face of the slab.

The COHORT data were a factor of 2 lower than the C-18 results and are normalized to the C-18 data at zero degrees. The same normalizing factor was used for both sets of COHORT calculations, so that a direct comparison between the two COHORT calculations may be made. The fact that the COHORT data were a factor of 2 lower than the C-18 calculation is not surprising when one realizes that in predicting the distribution of the flux within the slab, the COHORT prediction was lower by almost a factor of 2 near the outer edge of the slab. Aside from the magnitude, the scattered dose-rate curves calculated with the COHORT codes agree very well in shape, not only with each other but with the C-18 results.

There is some question about the true source term that should be used for these calculations. It is felt that there is not sufficient evidence to prove the COHORT calculations either right or wrong with the present data. General Dynamics will be using the COHORT codes in future work, and if there should be any errors detected in the codes, corrections will be made and notification of these corrections will be sent to MSFC.

III. CALCULATIONS FOR NERVA-TYPE GEOMETRY

An analysis of the neutron and gamma-ray fluxes leaking from a NERVA-type engine was intended to provide data to support the contention that the COHORT procedure will accurately predict the radiation through the complex geometries associated with the design of nuclear rockets. Unfortunately, checkout of the COHORT codes was not completed as early as previously planned, and a thorough analysis of the flux leakages from a NERVA-type engine was not possible in the time remaining after the completion of the checkout of the codes. Much of the preparatory work for the analysis of a NERVA-type engine was completed, however, and that information will be available if the need arises for a calculation of the flux leakages from the NERVA engine.

Geometry and cross-section data in the form required by the COHORT codes are on IBM cards at the Computations Laboratory (Bldg 4663), George C. Marshall Space Flight Center, Huntsville, Alabama. The gamma-ray cross sections and the geometry description are contained in the History-Generator Code problem deck labeled H019303, and the neutron cross sections and angular probability tables are contained in the deck labeled H019293. The cross sections available are those for the main elements that are contained in the materials composing the NERVA engine. Total, scattering, and elastic cross sections for neutrons and total, pair-production plus Compton, and Compton cross sections were tabulated for energies ranging from 0.2 to 10 Mev for each of the following elements:

hydrogen, lithium, beryllium, carbon, aluminum, titanium, iron, and uranium. The neutron cross sections for carbon and beryllium were taken from Reference 6. Neutron cross sections for iron and aluminum were taken from Reference 7. Lithium cross sections were taken from Reference 8. The Legendre expansion coefficients for the angular distributions of the elastically scattered neutrons were obtained for each of the above elements from the respective references and have been converted to angular cumulative probability distribution tables of the form required by the COHORT codes. Neutron total, scattering, and elastic cross sections for hydrogen, titanium, and uranium were obtained from Reference 9. The angular distribution for the elastically scattered neutrons from these elements were considered isotropic in the center-of-mass system for the NERVA test problems run thus far. This assumption was made for titanium and uranium simply because differential elastic cross sections were not available at the time the NERVA test problems were made out and because it was concluded that these two elements were not present in sufficient quantity that their angular scattering probabilities would have a determining effect on the dose rates leaking from the reactor.

The probabilities of exciting the nuclei to the various levels were not readily obtainable for all the elements. For beryllium, carbon, and lithium the assumption was made that all inelastic scattering would excite the first level of the target nucleus. Titanium was assumed to have the same excitation levels and the same probability of exciting those levels as does iron,

and it was assumed that there was no inelastic scattering with the uranium. These assumptions were made in order that a neutron problem might be run to check the portions of the code that read in the library rather than provide accurate results.

The geometry for a NERVA-type engine was described similar to the Computational Model in Reference 2. It was learned during the course of setting up the complex geometry that extreme care must be exercised in the geometric description so that no undefined regions exist in the geometry. Although the persons describing the geometry for the COHORT calculation were thoroughly familiar with the requirements and restrictions placed upon the geometry descriptions, several attempts were made before the geometry was successfully described. Even though the COHORT codes offer tremendous possibilities in geometry description, it would be advisable to always simplify the geometry as much as possible before trying to describe it.

A very rough calculation was made of the scattered gamma-ray fluxes at five positions on a radius 900 centimeters from the core center of a NERVA-type engine. Time did not allow a complete analysis of these data, but a quick comparison with calculations made with GD/FW's C-17 code and the Los Alamos Quad code indicates that the COHORT data are of the right order of magnitude. No attempt will be made to complete a more thorough analysis with the present data, because of the fact that these data were obtained during the checkout of the COHORT codes and do not offer as good statistics as could be obtained in a more detailed analysis of the flux leakage from the NERVA engine.

IV. RECOMMENDATIONS

Possibly the greatest advantage that the COHORT codes hold over similar flexible-geometry Monte Carlo codes is that the COHORT codes are written in the FORTRAN language. The fact that the codes are written in FORTRAN language does not necessarily mean that they are better than those written in machine language, but it does make readily available to engineers and technical persons having a reading knowledge of the FORTRAN language the detailed mechanics of the calculations performed by the codes. As one becomes familiar with the COHORT codes and the mechanics of the calculations performed, he will probably tend to modify the codes to improve their application to a particular problem or to use certain of the subroutines in the COHORT codes as subroutines in the development of newer codes.

There are two recommended additions to the COHORT codes that would improve their usefulness without requiring too much additional effort. These are that provision be made (1) for a means of checking the geometry input and (2) for a means of calculating a direct-beam flux at those detector positions at which the scattered fluxes are calculated with the Analysis Code, A01. It is possible that an additional code might be developed that would fulfill both of these recommendations.

First, a code that would calculate the direct-beam fluxes could be created almost in toto by lifting the necessary subroutines from the Analysis Code, A01, and by substituting as input a source tape rather than a history tape. In addition, an option could be provided that would print the thicknesses through each region measured

along lines joining a source point with each of the detector points and thus provide a means of checking the geometry input for a problem.

REFERENCES

1. Wells, M. B., and Malone, C. F., A Monte Carlo Procedure for Radiation Transport and Heating Studies. General Dynamics/Fort Worth Report FZK-156 (NAS8-1573, 29 October 1962). U
2. Standard NERVA Engine Analytical Model for Radiation Analysis. Aerojet General Corporation Report 2492 (February 1963). CRD
3. Burell, M. O., Nuclear Radiation Transfer and Heat Deposition Rates in Liquid Hydrogen. National Aeronautics and Space Administration Report NASA TN D-1115 (August 1962). U
4. Western, G. T., Energy and Angular Distribution Experiment. Volume I: Angular Distribution of Reactor Radiation from Slabs and of Emergent Secondary Gamma Rays. General Dynamics/Fort Worth Report FZK-9-183-1 (NARF-62-16T, 31 December 1962). U
5. Mooney, L. G., The Calculation of Fast-Neutron Attenuation Probabilities Through a Nine-Inch Polyethylene Slab and Comparison with Experimental Data. General Dynamics/Fort Worth Report FZM-2936 (10 June 1963). A paper presented at the American Nuclear Society Meeting, Salt Lake City, Utah, 17-19 June 1963.
6. Joanou, G. D., et al., Legendre Expansion Coefficients for the Angular Distribution of Elastically Scattered Neutrons and Fast-Neutron Cross Sections for Deuterium, Beryllium, Carbon, Oxygen, Zirconium, Lead, and Bismuth. General Dynamics/General Atomic Report GA-2156 (May 15, 1961). U
7. Troubetzkoy, E. S., Fast-Neutron Cross Sections of Iron, Silicon, Aluminum, and Oxygen. Nuclear Development Corporation of America Report NDA 2111-3 (17 December 1958-30 September 1959). U
8. Goldstein, H., and Aronson, R., Neutron Penetration in Lithium Compounds. Nuclear Development Corporation of America Report NDA 12-13 (January 20, 1955). CRD
9. Hughes, D. J., and Schwartz, R. B., Neutron Cross Sections. Brookhaven National Laboratory Report BNL 325 (1 July 1958).

DISTRIBUTION

Addressee

No. Copies

George C. Marshall Space Flight Center
National Aeronautics and Space Administration
Huntsville, Alabama
Attn: Procurement and Contract Office,
M-P & C-CA

12 plus re-
producibles.